UNIVERSITY OF LEEDS

This is a repository copy of *Combined Control of Morphology and Polymorph in Spray Drying of Mannitol for Dry Powder Inhalation*.

White Rose Research Online URL for this paper:
http://eprints.whiterose.ac.uk/114422/

Version: Accepted Version

**Article:**
Lyu, F, Liu, JJ, Zhang, Y et al. (1 more author) (2017) Combined Control of Morphology and Polymorph in Spray Drying of Mannitol for Dry Powder Inhalation. Journal of Crystal Growth, 467. pp. 155-161. ISSN 0022-0248

https://doi.org/10.1016/j.jcrysgro.2017.03.033

© 2017 Elsevier B.V. This manuscript version is made available under the CC-BY-NC-ND 4.0 license http://creativecommons.org/licenses/by-nc-nd/4.0/

**Reuse**
Unless indicated otherwise, fulltext items are protected by copyright with all rights reserved. The copyright exception in section 29 of the Copyright, Designs and Patents Act 1988 allows the making of a single copy solely for the purpose of non-commercial research or private study within the limits of fair dealing. The publisher or other rights-holder may allow further reproduction and re-use of this version - refer to the White Rose Research Online record for this item. Where records identify the publisher as the copyright holder, users can verify any specific terms of use on the publisher's website.

**Takedown**
If you consider content in White Rose Research Online to be in breach of UK law, please notify us by emailing eprints@whiterose.ac.uk including the URL of the record and the reason for the withdrawal request.

White Rose university consortium
Universities of Leeds, Sheffield & York

eprints@whiterose.ac.uk
https://eprints.whiterose.ac.uk/

Accepted Manuscript


# Combined Control of Morphology and Polymorph in Spray Drying of Mannitol for Dry Powder Inhalation

Feng Lyu, Jing J. Liu, Yang Zhang, Xue Z. Wang

PII: S0022-0248(17)30192-6
DOI: http://dx.doi.org/10.1016/j.jcrysgro.2017.03.033
Reference: CRYS 24108

To appear in: *Journal of Crystal Growth*

Received Date: 8 October 2016
Revised Date: 8 March 2017
Accepted Date: 20 March 2017

Please cite this article as: F. Lyu, J.J. Liu, Y. Zhang, X.Z. Wang, Combined Control of Morphology and Polymorph in Spray Drying of Mannitol for Dry Powder Inhalation, *Journal of Crystal Growth* (2017), doi: http://dx.doi.org/10.1016/j.jcrysgro.2017.03.033

This is a PDF file of an unedited manuscript that has been accepted for publication. As a service to our customers we are providing this early version of the manuscript. The manuscript will undergo copyediting, typesetting, and review of the resulting proof before it is published in its final form. Please note that during the production process errors may be discovered which could affect the content, and all legal disclaimers that apply to the journal pertain.

ACCEPTED MANUSCRIPT

# Combined Control of Morphology and Polymorph in Spray Drying of Mannitol for Dry Powder Inhalation

Feng Lyu[1], Jing J. Liu[2], Yang Zhang[1,*] and Xue Z. Wang[1,2,*]

[1]School of Chemistry and Chemical Engineering, South China University of Technology, Guangzhou, China 510640

[2]School of Chemical and Process Engineering, University of Leeds, Leeds LS2 9JT, U.K.

**Correspondence authors:**

Professor Xue Z. Wang
School of Chemistry and Chemical Engineering
South China University of Technology
381 Wushan Rd, Tianhe District
Guangzhou, PR China 510641
Email: xuezhongwang@scut.edu.cn
Tel: +86 20 8711 4000, Fax: +86 20 8711 4000
&
Professor Xue Z. Wang
Chair in Intelligent Measurement and Control
School of Chemical and Process Engineering
University of Leeds Leeds LS2 9JT, UK
Tel +44 113 343 2427, Fax +44 113 343 2384,
Email x.z.wang@leeds.ac.uk
Email: xuezhongwang@scut.edu.cn

Dr Yang Zhang
Lecturer
School of Chemistry and Chemical Engineering
South China University of Technology
381 Wushan Rd, Tianhe District
Guangzhou, PR China 510641
Tel: +86 20 8711 4000, Fax: +86 20 8711 4000
Email: ceyzhang@scut.edu.cn

ACCEPTED MANUSCRIPT

ACCEPTED MANUSCRIPT

**Abstract**

The morphology and polymorphism of mannitol particles were controlled during spray drying with the aim of improving the aerosolization properties of inhalable dry powders. The obtained microparticles were characterized using scanning electron microscopy, infrared spectroscopy, differential scanning calorimetry, powder X-ray diffraction and inhaler testing with a next generation impactor. Mannitol particles of varied α-mannitol content and surface roughness were prepared via spray drying by manipulating the concentration of $NH_4HCO_3$ in the feed solution. The bubbles produced by $NH_4HCO_3$ led to the formation of spheroid particles with a rough surface. Further, the fine particle fraction was increased by the rough surface of carriers and the high α-mannitol content. Inhalable dry powders with a 29.1 ± 2.4% fine particle fraction were obtained by spray-drying using 5% mannitol (w/v)/2% $NH_4HCO_3$ (w/v) as the feed solution, proving that this technique is an effective method to engineer particles for dry powder inhalation.

**Keywords:** A1. Morphology; A1. Polymorphism; A1. Heat transfer; A1. High resolution X-ray diffraction; A2. Spray drying; B1: Mannitol

ACCEPTED MANUSCRIPT

ACCEPTED MANUSCRIPT

## 1. Introduction

Inhalable medications are considered an effective therapy for the local treatment of diseases of the respiratory system such as asthma [1, 2]. In the preparation of inhalable medications, small particles of active pharmaceutical ingredients (API) are mixed with large carrier particles [3]. In order to aerosolize the drug particles, the properties of both the carriers and the API particles are of great importance since the drug–carrier adhesive forces need to be overcome by the patient's inspiratory force [4]. Studies have reported on the impact of particle mean size [5], particle size distribution [6], morphology [7, 8], crystal form [9], surface roughness [10] and surface energy [11] on the performance of inhalable dry powders. Indeed, the particle size, size distribution, morphology and polymorphism of carriers have been found to exert a major impact on the efficiency of dry powder inhalation (DPI) [12, 13], although results have not been consistent. For instance, Podczeck [14] found that small particles improved aerosol performance, while Kaialy et al. [5] observed that large particles had such an effect. Further, Maas et al. [15] and Kaialy et al. [16] found that smooth carriers provided a higher fine particle fraction (FPF) than rough carriers, while Littringer et al. [17] showed that rough surface carriers improved the FPF. Such inconsistencies may be attributed to the independent examination of individual properties rather than within the complete system. Nevertheless, the above mentioned studies emphasize the importance of drug carriers engineering in enhancing aerosol performance in DPI [18–20].

Mannitol has been chosen as the model excipient for this study in order to assess the combined control morphology and polymorphism of the carriers. Three crystal forms, α-, β- and δ-mannitol, have been approved as carriers of DPI. In addition, mannitol was found crystalline after spray drying [7]. However, little research has been performed on mannitol as a potential DPI drug delivery carrier [21].

ACCEPTED MANUSCRIPT

The polymorphism of materials is influenced by the operating conditions, the solvent mixture [22] and the additives [23] during the spray-drying process. Previous studies have reported that addition of insulin [24] and lysozyme [25] resulted in various mannitol polymorphisms following spray drying. Rough surface mannitol particles were prepared using Luria broth agar as an additive in an ethanol-water solvent [26]. Nevertheless, the toxicity following inhalation of these additives has not been adequately studied. Ideally, no residual additive should be present in the final mannitol product. $NH_4HCO_3$ has been previously examined as an additive for spray drying [27], and was found to decompose into $H_2O\uparrow$, $CO_2\uparrow$, and $NH_3\uparrow$ at temperatures above 50℃, leaving no additive residue after spray drying. Further, $NH_4HCO_3$ was seen to affect the morphology of drug particles during the spray-drying process [28].

Herein, control of both morphology and polymorphism was assessed in order to improve the aerosol properties of engineered particles and their DPI performance. Engineered mannitol particles were used as DPI carriers mixed with API budesonide. The effect of gas bubbles on particle morphology during droplet drying was studied using hot stage microscopy. Additionally, the influence of $NH_4HCO_3$ concentration was investigated.

## 2. Materials and methods

### 2.1 Materials

Columnar β-mannitol crystalline (≥99.0% HPLC) and $NH_4HCO_3$ were provided by Aladdin (Shanghai, China). Absolute ethanol was obtained from Nanjing Chemical Reagent Co., LTD, China. Micronized budesonide (YIXING, CHINA, $D_{10}$ = 1.10 ± 0.01 μm, $D_{50}$ = 1.98 ± 0.04 μm and $D_{90}$ = 4.59 ± 0.27 μm) was used as a model API for the adhesive mixtures.

### 2.2 Spray drying

ACCEPTED MANUSCRIPT

All particles were produced with a Buchi B-290 Mini spray dryer and inert loop B-295 organic solvents accessory. A 1.5-mm diameter nozzle screw cap and a 0.7-mm nozzle tip were used. When the organic solution was handled, the Buchi B-290 and B-295 were operated in closed mode. Nitrogen was used as the drying gas, heated to just below 200°C before being fed to the drying chamber. After the drying chamber, the nitrogen containing solvent vapours enters the condenser, where the solvent is condensed, while the cooled nitrogen is purged and is reheated again and fed to the drying camber to be used.

In all cases, a solution of 5% (w/v) mannitol in 25%:75% v/v ethanol:water was used. $NH_4HCO_3$ was then added and fully dissolved in the 5% (w/v) mannitol solution, before spray drying. The spray-drying process conditions were an air flow rate of 473 L/h, an aspirator rate of 100%, a mannitol solution feeding rate of 1.2 L/h, and an inlet temperature of 100℃. The spray-dried powders were collected in the hermetic bag and placed in glass desiccators at room temperature until further analysis. Formulations containing 0%, 1.67% and 2.00% of $NH_4HCO_3$, designated as samples A, B and C, respectively, were prepared by spray drying.

**2.3 Particle size, powder density, Carr index, Hausner ratio and theoretical aerodynamic diameter**

A Mastersizer 3000 equipped with a vacuum unit (Malvern, UK) was used to measure the particle size distribution of the engineered powders. The air pressure of the unit was set to 0.8 bars.

Bulk and tapped densities were tested according to the Chinese Standard Test Methods for Powder Characterization (GB/T 16913-2008) and for Powders Tap Density (GB/T21354-2008). Before bulk density was measured, the particles were placed in a drying oven for 8 hours at a constant temperature of 55℃, and were then filtered with an 80-mesh sieve. A 25 ml measuring cylinder (readable to 0.2 ml)

ACCEPTED MANUSCRIPT

loaded with 5.0g of the powder was tapped 2400 times; 2400 taps were sufficient to reach the maximum diminution in the particle bed volume. The value read from the measuring cylinder after tapping (tapped volume) was used to estimate the tapped densities. Each measurement was repeated three times, with the average value being reported.

The Carr index (CI) and Hausner ratio (H) are often used in the characterization of the flowability of particles; lower CI and H values imply better flowability [29, 30]. CI and H can be calculated from tap and bulk densities, $\rho_{tap}$ and $\rho_{bulk}$, using equations (1) and (2):

$$\mathrm{CI} = \frac{\rho_{tap} - \rho_{bulk}}{\rho_{tap}} \times 100\% \quad (1)$$

$$\mathrm{H} = \frac{\rho_{tap}}{\rho_{bulk}} \quad (2)$$

The theoretical primary aerodynamic diameter of the particles ($D_{ae}$) is estimated from the average particle size ($D_{50}$) and tapped density data ($\rho_{tap}$) using [31, 32]:

$$D_{ae} = D_{50}\sqrt{\frac{\rho_{tap}}{\rho_1}} \quad (3)$$

where $\rho_1 = 1$ g/cm$^3$

**2.4 Particle surface investigations**

The gold-palladium-coated powder samples were analysed by scanning electron microscopy (SEM) (Merlin, Zeiss, Germany).

**2.5 Hot stage microscopy**

The impact of gas bubbles on the particle surface roughness and morphology was investigated using a hot stage microscope. This was partly inspired by the work of Maas et al. [33], in which a hot stage was used to observe crystal growth behaviour within a liquid droplet. The hot stage used herein consisted of an Olympus BX53 microscope (Olympus, Japan) and a Linkam LNP95 hot stage reactor (Linkam, UK). A hydrophobic glass [34, 35] (no cover slip) was placed on the preheated (85℃) hot

ACCEPTED MANUSCRIPT

stage; after a few minutes, small droplets (2.6 mm in diameter) were prepared using a microliter syringe from the 5% (w/v) mannitol solution (samples A, B and C) and placed on the glass (one at a time). The drying and crystallization processes were directly observed using the Olympus BX53 microscope with a CCD camera. Image-pro plus software was used for image analysis.

**2.6 Powder X-ray diffraction (XRD)**

A D8 Advance X-ray diffractometer (Bruker Corporation, Germany) was used for the assessment of the polymorphic forms of the commercial mannitol and all engineered powders. The samples were collected on a stainless steel holder. The surface of the powders was flattened manually for analysis. Each sample was scanned from 5° to 40° of 2θ, with a step size of 0.01° per second.

**2.7 Detection of residual of additives**

Infrared spectroscopy (ReactIR$^{TM}$15, Mettler-Toledo, Switzerland) was used to detect the existence of $NH_4HCO_3$ in the spray-dried mannitol particles.

**2.8 Homogeneity testing**

Budesonide was mixed with the carrier at a carrier to drug weight ratio of 99:1 using a whirlpool mixer for 15 min. Each powder sample (20 ± 5 mg) was placed in the capsules (size 3) to yield a nominal dose of 200 ± 10 μg budesonide per capsule (content uniformity of formulations was evaluated). Homogeneity testing was performed to assess the homogenous content of budesonide through analysis of three random samples (20 ± 5 mg powder, 200 ± 10 μg budesonide per capsule). The powder was dissolved in 25 mL of an ethanol:water mixture (25%:75% v/v) and was assayed by ultraviolet (UV) spectrophotometry (UV mini-1240, Shimadzu, Japan) at 247 nm [26].

**2.9 In vitro aerosolization and deposition properties**

The deposition and in vitro aerosolization properties were measured using a Next Generation Impactor

ACCEPTED MANUSCRIPT

(NGI, Copley Scientific, USA). In each test, the air flow rate was adjusted to 60 L/min. In each experiment, ten capsules (20 ± 5 mg powder, 200 ± 10 μg budesonide) were individually installed in a Cyclohaler® device. A 25%:75% v/v ethanol:water solution was used as the collection fluid at the impinger stages. Each section was rinsed with the collection solvent and the exact amount of the drug in solutions was then assayed by UV spectrophotometry at 247 nm.

The recovered dose was the total amount of the drug recovered from the capsule, the inhaler device, the pre-separator, the induction port and all stages of the impactor. The amount of budesonide deposited in stages S2, S3, S4, S5, S6, S7 and Moc of the impinger was considered as the fine particle dose. The FPF was determined as the ratio of fine particle dose to recovered dose [22].

**2.10 Differential scanning calorimetry (DSC)**

Thermal analysis was conducted with a differential scanning calorimeter (Diamond DSC, PerkinElmer, USA) using a 9-mg sample, at a heating rate of 10 K/min from 30℃ to 300℃, under an argon atmosphere (50 mL/min).

**2.11 Wetting angle of the droplets**

Small droplets were prepared under the same condition with the hot stage microscopy experiment and were placed on the hydrophobic glass. The wetting angle of the droplets was measured using a Dataphysics (OCA40 Micro, DataPhysics, Germany).

**3. Results and discussion**

**3.1 Microparticle properties and process parameters**

The average particle size, the aerodynamic diameter, the tap and bulk density, CI, H and FPF of spray-dried mannitol particles are listed in Table 1. The average particle sizes for samples A, B and C ranged from 9.58 μm to 12.4 μm. Engineered mannitol particles had a significantly lower average

ACCEPTED MANUSCRIPT

particle size and tap and bulk density compared to commercial mannitol. The tap and bulk densities increased with increasing concentration of $NH_4HCO_3$. Further, the measured values of CI (>40%) and H (>1.6) indicate an extremely poor flow ability [17, 36]; however, commercial mannitol and spray-dried mannitol had similarly poor flow properties. The measured outlet temperature was 65°C, and did not change with the concentration of $NH_4HCO_3$ in the feed solution.

### 3.2 Testing the $NH_4HCO_3$ in spray-dried mannitol

The IR spectra of commercial mannitol showed peaks at 1025.82, 1081.21, 1421.13 and 1637.96 $cm^{-1}$ (Fig. 1). $NH_4HCO_3$ has a characteristic peak at 1700 $cm^{-1}$ indicating the presence of C=O bond. Interestingly, samples A, B and C (Fig. 1) showed the characteristic peaks of mannitol and no peak at 1700 $cm^{-1}$, indicating that $NH_4HCO_3$ was completely decomposed during spray drying and therefore was not present in the final products.

### 3.3 Drug content homogeneity

The drug content and the coefficient of variation for each capsule are provided in Table 2. Since the coefficient of variation for all four capsules was less than 8%, it was assumed that the blends were uniform [37–39].

### 3.4 Morphology

SEM images show the mannitol crystals on the surface of the engineered mannitol microparticles (Fig. 2I). Using ImageJ software, a rectangular area (3.7×5.1 μm) on the centre of each particle was transformed into 2D and 3D surface plots for samples A, B and C (Fig. 2Ⅱ and Ⅲ, respectively). Sample A mannitol microparticles were observed to have a relatively smooth surface (as depicted by the green area in the 2D and 3D plots) with deposited fine needle crystals and small particles (Fig. 2a). On the other hand, sample B microparticles had an irregular surface, as denoted by the blue area in the

ACCEPTED MANUSCRIPT

2D and 3D plots (Fig. 2b). Finally, sample C microparticles had an irregular structure and rough surface due to the formation of large crystals (Fig. 2c), as observed by the increased blue area coverage in the 2D and 3D plots compared to the previous two samples. Therefore, the concentration of $NH_4HCO_3$ in the mannitol solution had a significant influence on the morphology of spray-dried mannitol particles. This phenomenon is different from what was reported by Ali et al. [28]. Ali et al. did not observe morphological changes with increasing $NH_4HCO_3$ concentration. The reason that the findings here differ from Ali et al. is probably due to the difference in operational conditions between our work and that of Ali et al. in terms of inlet temperature and concentration. In the work of Ali et al., the temperature of the inlet gas was from 110℃ to 170℃, and the concentrations of mannitol and NH4HCO3. were from 10% to 70% and 5% to 20% respectively. It is known that the inlet temperature of the drying gas was related to the decomposition rate of NH4HCO3, and increased concentration of the feed solution could lead to increased solid content of spray dried particles.

$NH_4HCO_3$, which decomposes into gas bubbles during the drying process, was used as a pore former to change the particle morphology. The morphology of particles can be strongly influenced by the formation of bubbles in relation to the initial nucleation within the droplets [40]. Various methods to investigate single droplet drying mechanisms have been reported, such as using a glass filament [41], hydrophobic surfaces [34], acoustic levitation [42–44], aerodynamic levitation [45] and leidenfrost drop forms [20, 46, 47]. Herein, hot stage microscopy was employed, wherein a hydrophobic surface was created to investigate the impact of gas bubbles on the morphology of the spray-dried particles. In the drying process for samples A, B and C can be observed in Fig. 3a, b and c, respectively. The droplet diameter decreased for several seconds until recrystallization commenced. Bubbles appeared in the droplets of samples B and C at 37 and 35 seconds, respectively (Fig. 3b and c), inflating and

ACCEPTED MANUSCRIPT

rupturing quickly. The number of mannitol crystals formed increased rapidly following bubble formation. On the other hand, the sample A droplet shrunk quickly due to the fast solvent evaporation but remained liquid and did not recrystallize. Crystals emerged after 45 seconds (Fig. 3a), and grew fast. At the same time, the droplets for samples B (Fig. 3b) and C (Fig. 3c) were covered by mannitol crystals. It is worth noting that the solute may not instantly crystallize while the saturation is satisfied at the surface of the droplet. Interestingly, the rate of nucleation and crystal growth determine the time to crystallization in the solution [48]. Indeed, gas bubbles can have a positive effect on crystallization, as commented by Nakamura [49], Matsumoto [50] and Deora [51]. During bubble formation and rupture, several processes may trigger crystallization. For instance, the inflation and rupture of the cavitation bubbles may cause transient pressure due to dramatic changes in the pressure, possibly leading to improved crystallization [52]. It is speculated that a similar cavitation phenomenon during hot stage microscopy might occur during spray-drying, but this cannot be validated at present since it is hard to observe experimentally during the spray drying process. However, the morphology and size of mannitol crystals within the particle are difficult to observe through the microscope since the wetting angle of droplets (A, B and C) on hydrophobic glass slide are in the range of 93° to 98° and the mannitol crystals overlap to compose the particle. Hence, the relationship between the morphology of mannitol crystals and the roughness of the mannitol particles is not yet clear. On the other hand, the particles appear irregular spheroidal since internal bubbles escape violently from the film of droplets [40, 53]. With the increase in $NH_4HCO_3$ concentration, a large number of minute bubbles were observed to break through the droplet film or particle shell. Furthermore, too many bubbles led to unstable droplets that easily broke and coalesced. At $NH_4HCO_3$ concentrations above 2.0%, the particles had an extremely irregular shape and were agglomerated.

ACCEPTED MANUSCRIPT

### 3.5 Investigation on polymorphism

The DSC curves of all samples as well as commercial mannitol (Fig. 4) revealed a single melting peak at 168.9 ± 1℃, indicating the presence of either α-mannitol or β-mannitol [36]; no melting events appeared in the DSC curve at approximately 155℃ (the melting point of δ-mannitol). Therefore, the presence of δ-mannitol was excluded. The XRD pattern of commercial mannitol corresponded to β-mannitol, but all three spray-dried samples were a mixture of α- and β-mannitol. The peaks at 9.4°, 13.8° and 17.4° of 2θ indicated the presence of α-mannitol, while the peaks at 10.6°, 14.7° and 16.8° of 2θ indicated the presence of β-mannitol [26]. With regards to the height of peaks at 13.8° (α) and 14.7° (β) (Fig. 5), the peak intensity of sample A was greater at 14.7° (β) compared to C, but lower at 13.8° (α) compared to C; a similar pattern was observed for peaks at 16.8° (β) and 17.4° (α). Therefore, the proportion of α-mannitol increased with increasing $NH_4HCO_3$ concentration. Quantitative analysis of the XRD data [54, 55] was applied to calculate the content of α-mannitol. The α-mannitol content in samples A, B and C was 4.76%, 44.55% and 59.86%, respectively (Fig. 6). Therefore, spray-dried mannitol was composed of a mixture of α-mannitol and β-mannitol, in agreement with previous findings [28, 33]. Interestingly, variations in the concentration of $NH_4HCO_3$, as well as changes in the outlet temperature [28] and the concentration of the mannitol solution [33], leads to control of the α- and β-mannitol ratio. Moreover, the use of ethanol also favoured the formation of α-mannitol, since an ethanol-water system has a higher drying rate compared to pure water under the same drying conditions [9, 56].

### 3.6 In vitro deposition properties

As shown in Table 1, all engineered microparticles provided a sharply higher FPF for inhalable dry powders than commercial mannitol, likely due to changes in the properties of commercial mannitol,

ACCEPTED MANUSCRIPT

such as density and aerodynamic diameter, following spray drying. Furthermore, the FPF increased with increasing concentration of $NH_4HCO_3$ in the feed solution; sample C had the highest FPF (29.1 ± 2.4%) among the four samples. It is likely that both the rough surface and the high percentage of α-mannitol contributed to this high FPF. Previous studies reported that rough surfaced carriers had an enhanced DPI performance [10, 17, 57]. Additionally, α-mannitol generates more cohesive and adhesive powders due to its high dispersive surface energy (74.9 $mJm^{-2}$) compared to that of β-mannitol (40.0 $mJm^{-2}$) [48]. Tang et al. [58] concluded that high surface energies in powders lead to an improvement in the respirable fractions of the API. The FPF of inhalable dry powders is affected by many factors, including size, polymorphism and morphology, which together influence aerosol performance. The proposed synthesis method controls the morphology and the polymorph of mannitol particles by altering the concentration of $NH_4HCO_3$ in the feed solution during spray drying.

**4. Conclusion**

$NH_4HCO_3$ was found to form mannitol particles with rough surfaces and spheroid shape when used as an additive in the spray-drying process. Furthermore, gas bubbles formed by the decomposition of $NH_4HCO_3$ were found to have a positive effect on the crystallization of mannitol during the droplet drying process. The concentration of $NH_4HCO_3$ in the mannitol solution significantly affected the particle aerodynamic diameter, morphology and polymorphic properties. The proportion of α-mannitol increased from 4.76% to 59.86% with increasing concentration of $NH_4HCO_3$. In addition, $NH_4HCO_3$ was not detected in spray-dried mannitol particles, indicating its complete decomposition during the spray-drying process. Increasing the proportion of α-mannitol, leading to high dispersion surface energy and rough surface particles contributed to increasing the FPF. The highest FPF of 29.1 ± 2.4%

ACCEPTED MANUSCRIPT

was achieved using 5.00% w/v of mannitol and 2.00% w/v of $NH_4HCO_3$, which had the highest surface roughness and α-mannitol fraction.

## References

[1] G. Pilcer, N. Wauthoz, K. Amighi, Lactose characteristics and the generation of the aerosol, Advanced Drug Delivery Reviews, 64 (2012) 233-256.
[2] N. Labiris, M. Dolovich, Pulmonary drug delivery. Part I: physiological factors affecting therapeutic effectiveness of aerosolized medications, British Journal of Clinical Pharmacology, 56 (2003) 588-599.
[3] S. Karner, M. Maier, E. Littringer, N.A. Urbanetz, Surface roughness effects on the tribo-charging and mixing homogeneity of adhesive mixtures used in dry powder inhalers, Powder Technology, 264 (2014) 544-549.
[4] V. Berard, E. Lesniewska, C. Andres, D. Pertuy, C. Laroche, Y. Pourcelot, Dry powder inhaler: influence of humidity on topology and adhesion studied by AFM, International Journal of Pharmaceutics, 232 (2002) 213-224.
[5] W. Kaialy, A. Alhalaweh, S.P. Velaga, A. Nokhodchi, Influence of lactose carrier particle size on the aerosol performance of budesonide from a dry powder inhaler, Powder Technology, 227 (2012) 74-85.
[6] A. Khalil, F. Puel, X. Cosson, O. Gorbatchev, Y. Chevalier, J.-M. Galvan, A. Rivoire, J.-P. Klein, Crystallization-in-emulsion process of a melted organic compound: in situ optical monitoring and simultaneous droplet and particle size measurements, Journal of Crystal Growth, 342 (2012) 99-109.
[7] E.M. Littringer, M.F. Noisternig, A. Mescher, H. Schroettner, P. Walzel, U.J. Griesser, N.A. Urbanetz, The morphology and various densities of spray dried mannitol, Powder Technology, 246 (2013) 193-200.
[8] W. Kaialy, G.P. Martin, H. Larhrib, M.D. Ticehurst, E. Kolosionek, A. Nokhodchi, The influence of physical properties and morphology of crystallised lactose on delivery of salbutamol sulphate from dry powder inhalers, Colloids and Surfaces B: Biointerfaces, 89 (2012) 29-39.
[9] Y.-Y. Lee, J.X. Wu, M. Yang, P.M. Young, F. van den Berg, J. Rantanen, Particle size dependence of polymorphism in spray-dried mannitol, European Journal of Pharmaceutical Sciences, 44 (2011) 41-48.
[10] S. Karner, E.M. Littringer, N.A. Urbanetz, Triboelectrics: the influence of particle surface roughness and shape on charge acquisition during aerosolization and the DPI performance, Powder Technology, 262 (2014) 22-29.
[11] D. Cline, R. Dalby, Predicting the quality of powders for inhalation from surface energy and area, Pharmaceutical Research, 19 (2002) 1274-1277.
[12] B. Zhu, D. Traini, D.A. Lewis, P. Young, The solid-state and morphological characteristics of particles generated from solution-based metered dose inhalers: Influence of ethanol concentration and intrinsic drug properties, Colloids & Surfaces A Physicochemical & Engineering Aspects, 443 (2014) 345-355.
[13] C.W. Park, X. Li, F.G. Vogt, H.D. Jr, J.B. Zwischenberger, E.S. Park, H.M. Mansour, Advanced spray-dried design, physicochemical characterization, and aerosol dispersion performance of vancomycin and clarithromycin multifunctional controlled release particles for targeted respiratory delivery as dry powder inhalation aerosols, International Journal of Pharmaceutics, 455 (2013) 374-392.
[14] F. Podczeck, The relationship between physical properties of lactose monohydrate and the aerodynamic behaviour of adhered drug particles, International Journal of Pharmaceutics, 160 (1998) 119-130.
[15] S.G. Maas, G. Schaldach, P. Walzel, N.A. Urbanetz, Tailoring dry powder inhaler performance by modifying carrier surface topography by spray drying, Atomization and Sprays, 20 (2010) 763-774.
[16] W. Kaialy, A. Nokhodchi, Freeze-dried mannitol for superior pulmonary drug delivery via dry powder inhaler,

ACCEPTED MANUSCRIPT

Pharmaceutical Research, 30 (2013) 458-477.
[17] E.M. Littringer, A. Mescher, H. Schroettner, L. Achelis, P. Walzel, N.A. Urbanetz, Spray dried mannitol carrier particles with tailored surface properties – the influence of carrier surface roughness and shape, European Journal of Pharmaceutics and Biopharmaceutics, 82 (2012) 194-204.
[18] W. Kaialy, M.N. Momin, M.D. Ticehurst, J. Murphy, A. Nokhodchi, Engineered mannitol as an alternative carrier to enhance deep lung penetration of salbutamol sulphate from dry powder inhaler, Colloids and Surfaces B: Biointerfaces, 79 (2010) 345-356.
[19] H.-K. Chan, N.Y. Chew, Novel alternative methods for the delivery of drugs for the treatment of asthma, Advanced Drug Delivery Reviews, 55 (2003) 793-805.
[20] Lintingre, G. Ducouret, F. Lequeux, L. Olanier, T. Périé, L. Talini, Controlling the buckling instability of drying droplets of suspensions through colloidal interactions, Soft Matter, 11 (2015) 3660-3665.
[21] W. Kaialy, H. Larhrib, M. Ticehurst, A. Nokhodchi, Influence of Batch Cooling Crystallization on Mannitol Physical Properties and Drug Dispersion from Dry Powder Inhalers, Crystal Growth & Design, 12 (2012) 3006-3017.
[22] R. Sarrate, J.R. Ticó, M. Miñarro, C. Carrillo, A. Fàbregas, E. García-Montoya, P. Pérez-Lozano, J.M. Suñé-Negre, Modification of the morphology and particle size of pharmaceutical excipients by spray drying technique, Powder Technology, 270 (2015) 244-255.
[23] A.B.D. Nandiyanto, K. Okuyama, Progress in developing spray-drying methods for the production of controlled morphology particles: from the nanometer to submicrometer size ranges, Advanced Powder Technology, 22 (2011) 1-19.
[24] H. Hamishehkar, J. Emami, K. Gilani, M. Minaiyan, H. Mahdavi, A. Nokhodchi, Influence of carrier particle size, carrier ratio and addition of fine ternary particles on the dry powder inhalation performance of insulin-loaded PLGA microcapsules, Powder Technology, 201 (2010) 289-295.
[25] H. Grohganz, Y.-Y. Lee, J. Rantanen, M. Yang, The influence of lysozyme on mannitol polymorphism in freeze-dried and spray-dried formulations depends on the selection of the drying process, International Journal of Pharmaceutics, 447 (2013) 224-230.
[26] F. Zhang, N.T.Q. Ngoc, B.H. Tay, A. Mendyk, Y.-H. Shao, R. Lau, Roughness-controlled self-assembly of mannitol/LB agar microparticles by polymorphic transformation for pulmonary drug delivery, Molecular Pharmaceutics, 12 (2015) 223-231.
[27] C. Gervelas, A.-L. Serandour, S. Geiger, G. Grillon, P. Fritsch, C. Taulelle, B. Le Gall, H. Benech, J.-R. Deverre, E. Fattal, Direct lung delivery of a dry powder formulation of DTPA with improved aerosolization properties: effect on lung and systemic decorporation of plutonium, Journal of Controlled Release, 118 (2007) 78-86.
[28] A. Al-Khattawi, J. Koner, P. Rue, D. Kirby, Y. Perrie, A. Rajabi-Siahboomi, A.R. Mohammed, A pragmatic approach for engineering porous mannitol and mechanistic evaluation of particle performance, European Journal of Pharmaceutics and Biopharmaceutics, 94 (2015) 1-10.
[29] M. Jaimini, A. Rana, Y. Tanwar, Formulation and evaluation of famotidine floating tablets, Current Drug Delivery, 4 (2007) 51-55.
[30] T.P. Learoyd, J.L. Burrows, E. French, P.C. Seville, Chitosan-based spray-dried respirable powders for sustained delivery of terbutaline sulfate, European Journal of Pharmaceutics and Biopharmaceutics, 68 (2008) 224-234.
[31] C. Bosquillon, C. Lombry, V. Preat, R. Vanbever, Influence of formulation excipients and physical characteristics of inhalation dry powders on their aerosolization performance, J Control Release, 70 (2001) 329-339.
[32] M.I. Amaro, F. Tewes, O. Gobbo, L. Tajber, O.I. Corrigan, C. Ehrhardt, A.M. Healy, Formulation, stability and

ACCEPTED MANUSCRIPT

pharmacokinetics of sugar-based salmon calcitonin-loaded nanoporous/nanoparticulate microparticles (NPMPs) for inhalation, International Journal of Pharmaceutics, 483 (2015) 6-18.
[33] S.G. Maas, G. Schaldach, E.M. Littringer, A. Mescher, U.J. Griesser, D.E. Braun, P.E. Walzel, N.A. Urbanetz, The impact of spray drying outlet temperature on the particle morphology of mannitol, Powder Technology, 213 (2011) 27-35.
[34] J. Perdana, M.B. Fox, M.A.I. Schutyser, R.M. Boom, Single-Droplet Experimentation on Spray Drying: Evaporation of a Sessile Droplet, Chemical Engineering & Technology, 34 (2011) 1151-1158.
[35] A.L. Biance, C. Clanet, D. Quéré, First steps in the spreading of a liquid droplet, Physical Review E Statistical Nonlinear & Soft Matter Physics, 69 (2004) 383-391.
[36] W. Kaialy, A. Nokhodchi, Dry powder inhalers: physicochemical and aerosolization properties of several size-fractions of a promising alterative carrier, freeze-dried mannitol, European Journal of Pharmaceutical Sciences, 68 (2015) 56-67.
[37] M.-P. Flament, P. Leterme, A. Gayot, The influence of carrier roughness on adhesion, content uniformity and the in vitro deposition of terbutaline sulphate from dry powder inhalers, International Journal of Pharmaceutics, 275 (2004) 201-209.
[38] M.D. Louey, M. Van Oort, A.J. Hickey, Aerosol dispersion of respirable particles in narrow size distributions using drug-alone and lactose-blend formulations, Pharmaceutical Research, 21 (2004) 1207-1213.
[39] H. Larhrib, G.P. Martin, C. Marriott, D. Prime, The influence of carrier and drug morphology on drug delivery from dry powder formulations, International Journal of Pharmaceutics, 257 (2003) 283-296.
[40] D. Walton, C. Mumford, The morphology of spray-dried particles: the effect of process variables upon the morphology of spray-dried particles, Chemical Engineering Research and Design, 77 (1999) 442-460.
[41] S. Yamamoto, Y. Sano, Drying of enzymes: enzyme retention during drying of a single droplet, Chemical Engineering Science, 47 (1992) 177-183.
[42] A.L. Yarin, G. Brenn, J. Keller, M. Pfaffenlehner, E. Ryssel, C. Tropea, Flowfield characteristics of an aerodynamic acoustic levitator, Physics of Fluids, 9 (1997) 3300-3314.
[43] S. Basu, E. Tijerino, R. Kumar, Insight into morphology changes of nanoparticle laden droplets in acoustic field, Applied Physics Letters, 102 (2013) 141602-141602-141605.
[44] W.K. Rhim, S.K. Chung, M.T. Hyson, E.H. Trinh, Large Charged Drop Levitation Against Gravity, IEEE Transactions on Industry Applications, IA-23 (1987) 975-979.
[45] A.S. Gandhi, A. Saravanan, V. Jayaram, Containerless processing of ceramics by aerodynamic levitation, Materials Science & Engineering A, 221 (1996) 68-75.
[46] A.L. Biance, C. Clanet, D. Quéré, Leidenfrost drops, Physics of Fluids (1994-present), 15 (2003) 1632-1637.
[47] N. Tsapis, E.R. Dufresne, S.S. Sinha, C.S. Riera, J.W. Hutchinson, L. Mahadevan, D.A. Weitz, Onset of buckling in drying droplets of colloidal suspensions, Physical Review Letters, 94 (2005) 018302-018302.
[48] M.G. Cares-Pacheco, G. Vaca-Medina, R. Calvet, F. Espitalier, J.J. Letourneau, A. Rouilly, E. Rodier, Physicochemical characterization of d-mannitol polymorphs: the challenging surface energy determination by inverse gas chromatography in the infinite dilution region, International Journal of Pharmaceutics, 475 (2014) 69-81.
[49] K. Nakamura, Y. Hosokawa, H. Masuhara, Anthracene crystallization induced by single-shot femtosecond laser irradiation: experimental evidence for the important role of bubbles, Crystal Growth & Design, 7 (2007) 885-889.
[50] M. Matsumoto, T. Fukunaga, K. Onoe, Polymorph control of calcium carbonate by reactive crystallization using microbubble technique, Chemical Engineering Research and Design, 88 (2010) 1624-1630.
[51] N. Deora, N. Misra, A. Deswal, H. Mishra, P. Cullen, B. Tiwari, Ultrasound for improved crystallisation in

ACCEPTED MANUSCRIPT

food processing, Food Engineering Reviews, 5 (2013) 36-44.
[52] M. Frenz, F. Konz, H. Pratisto, H.P. Weber, Starting mechanisms and dynamics of bubble formation induced by a Ho:Yttrium aluminum garnet laser in water, Journal of Applied Physics, 84 (1998) 5905-5912.
[53] E.M. Littringer, R. Paus, A. Mescher, H. Schroettner, P. Walzel, N.A. Urbanetz, The morphology of spray dried mannitol particles — the vital importance of droplet size, Powder Technology, 239 (2013) 162-174.
[54] H. Zhang, J.F. Banfield, Understanding polymorphic phase transformation behavior during growth of nanocrystalline aggregates: insights from TiO2, The Journal of Physical Chemistry B, 104 (2000) 3481-3487.
[55] S.N. Campbell Roberts, A.C. Williams, I.M. Grimsey, S.W. Booth, Quantitative analysis of mannitol polymorphs. X-ray powder diffractometry—exploring preferred orientation effects, Journal of Pharmaceutical and Biomedical Analysis, 28 (2002) 1149-1159.
[56] W. Ostwald, Studien uber die bildung und umwandlung fester korper, Z. Phys. Chem, 22 (1897) 289-330.
[57] T.Q.N. Nguyen, H.L. Giam, Y. Wang, A. Pacławski, J. Szlęk, A. Mendyk, Y.-H. Shao, R. Lau, Surface modification of pollen-shape carriers for dry powder inhalation through surface etching, Industrial & Engineering Chemistry Research, 53 (2014) 19943-19950.
[58] P. Tang, H.K. Chan, H. Chiou, K. Ogawa, M.D. Jones, H. Adi, G. Buckton, R.K. Prud Homme, J.A. Raper, Characterisation and aerosolisation of mannitol particles produced via confined liquid impinging jets, International Journal of Pharmaceutics, 367 (2009) 51-57.

ACCEPTED MANUSCRIPT

ACCEPTED MANUSCRIPT

## Tables and Figures

### Table 1

Micromeritic properties of spray-dried mannitol*

| Sample | $D_{50}$ (μm) | $D_{ae}$ (μm) | $\rho_{tap}$ (g/cm$^3$) | $\rho_{bulk}$ (g/cm$^3$) | H | CI | FPF (%) | Tout (°C) |
|---|---|---|---|---|---|---|---|---|
| CM | 109 | 86.7 | 0.63 | 0.33 | 1.9 | 0.5 | 7.5±0.4 | - |
| A | 9.58 | 5.41 | 0.32 | 0.14 | 2.4 | 0.6 | 18.8±0.8 | 65 |
| B | 10.5 | 6.4 | 0.37 | 0.16 | 2.3 | 0.6 | 20.1±1.1 | 65 |
| C | 12.4 | 7.8 | 0.40 | 0.20 | 2.0 | 0.5 | 29.1±2.4 | 65 |

* CI – Carr index, defined by eq. (1); H - Hausner ratio, defined by eq. (2) and FPF – fine particle fraction

* CM – commercial mannitol

### Table 2

Budesonide content and homogeneity of the blends*

| Blend | Run1 (%) | Run2 (%) | Run3 (%) | Average (%) | CV (%) |
|---|---|---|---|---|---|
| CM | 0.99 | 1.00 | 0.99 | 0.99 | 0.93 |
| A | 1.01 | 1.01 | 1.02 | 1.02 | 0.53 |
| B | 1.02 | 1.03 | 1.05 | 1.03 | 1.21 |
| C | 1.05 | 1.05 | 1.05 | 1.05 | 0.89 |

* CM – commercial mannitol; CV - coefficient of variation

ACCEPTED MANUSCRIPT

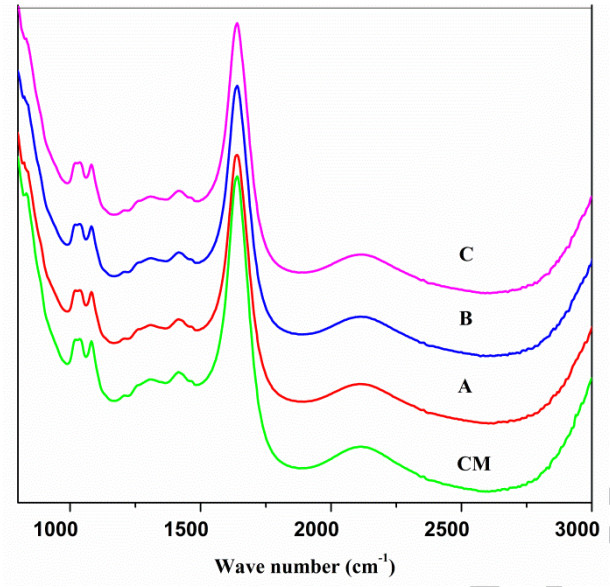


**Fig. 1.** Infrared spectrum for spray dried mannitol with different concentration of $NH_4HCO_3$, commercial mannitol (CM), A-0%, B-1.67%, C-2.00%.

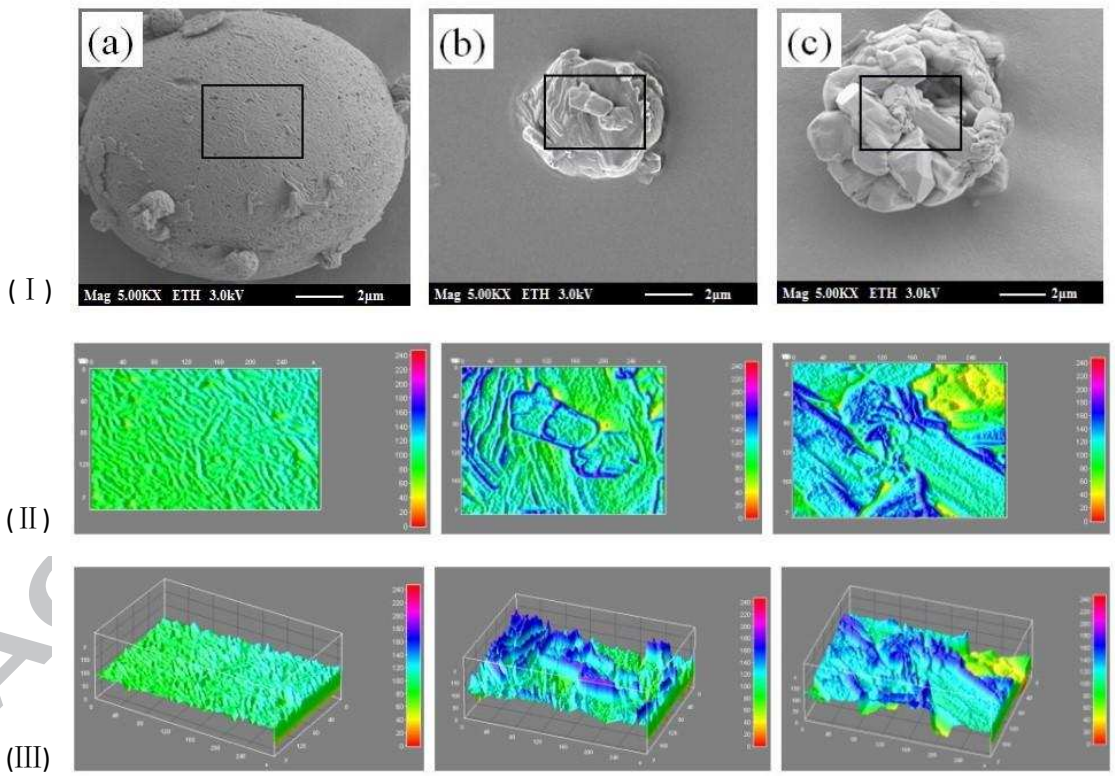


**Fig. 2.** SEM micrographs of mannitol samples spray dried at different concentration of $NH_4HCO_3$, (a)A-0%, (b) B-1.67%,(c) C-2.00%; (Ⅰ) SEM, (Ⅱ) 2D plot, (Ⅲ) 3D plot.

ACCEPTED MANUSCRIPT

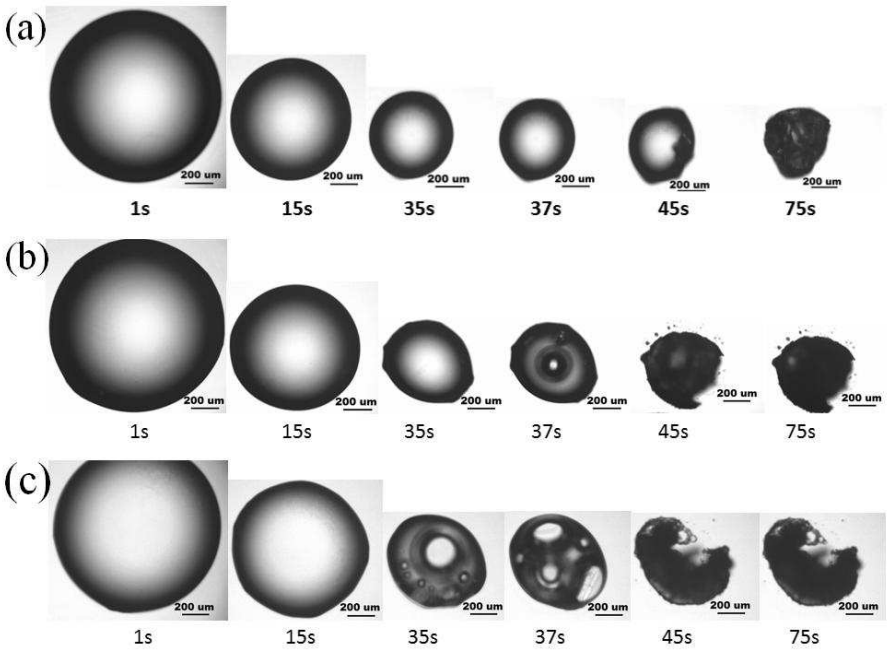


**Fig. 3.** The effect of bubbles on crystallization of mannitol during droplet drying, (a) A-0%, (b) B-1.67%, (c) C-2.00%.

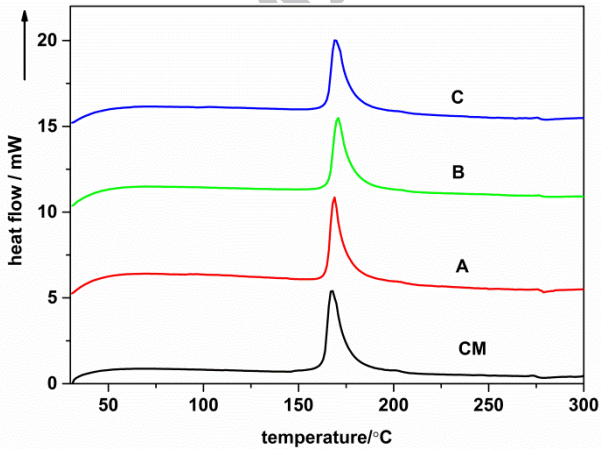


**Fig. 4.** DSC traces of mannitol samples commercial mannitol (CM), A-0%, B-1.67% and C-2.00%. Heating rate: 10K/min. one tick mark of the y-axis represents 22 mW.

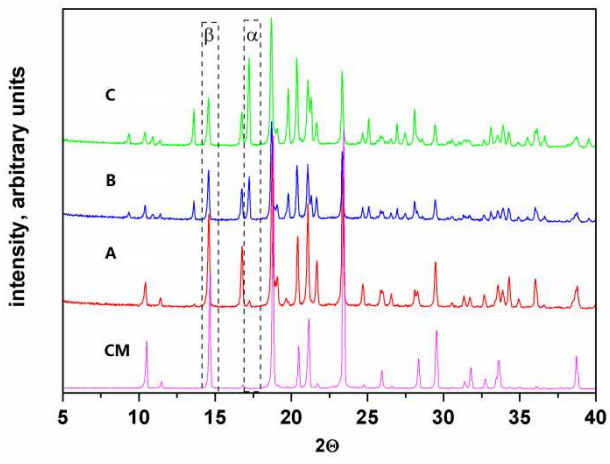

ACCEPTED MANUSCRIPT

**Fig. 5.** XRPD for spray dried mannitol with different concentration of $NH_4HCO_3$: commercial mannitol (CM), A-0%, B-1.67%, C-2.00%.

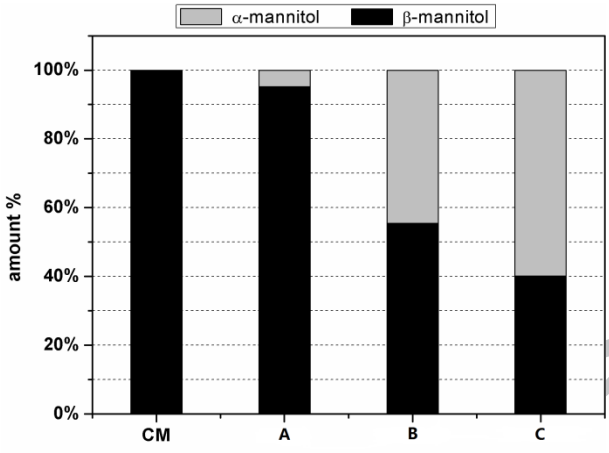


**Fig. 6.** Proportion of α-mannitol polymorphs in samples of commercial mannitol (CM), A-0%, B-1.67%, C-2.00%.

ACCEPTED MANUSCRIPT

ACCEPTED MANUSCRIPT

## Highlights

1. Mannitol particle morphology and polymorph are controlled by $NH_4HCO_3$ and mixture solvent.
2. Surface roughness and polymorphism are determined by concentration of $NH_4HCO_3$.
3. The rough surface and α mannitol increased the fine particle fraction of inhalation dry powders.
4. Bubbles improved the nucleation and growth of mannitol crystals.

ACCEPTED MANUSCRIPT